Astron. Astrophys. 349, 898–906 (1999)

ASTRONOMY AND ASTROPHYSICS

Tip-AGB stellar evolution in the presence of a pulsating, dust-induced "superwind"

K.-P. Schröder, J.M. Winters, and E. Sedlmayr

Technische Universität Berlin, Institut für Astronomie und Astrophysik, Sekr. PN 8-1, Hardenbergstrasse 36, D-10623 Berlin, Germany

Received 29 January 1998 / Accepted 3 August 1999

Abstract. We present selected "superwind" mass-loss histories and the related tip-AGB stellar evolution models, which have been computed according to the characteristics of a dust-induced, carbon-rich wind, and which include several recent improvements as compared to Schröder et al. (1998). We discuss the (initial) stellar mass-range of 1 to 2.5 $M_\odot$, with a nearly solar composition (X=0.28, Y=0.70, Z=0.02). In each time-step, mass-loss rates are used, which are consistent with the actual stellar parameters, and which are based on our pulsating, dust-induced wind models for carbon-rich stars (Fleischer et al. 1992), including a detailed and consistent treatment of dust formation, radiative transfer and radiative wind acceleration.

The resulting "superwind" mass-loss rates reach 2 to $3 \cdot 10^{-5} M_\odot$ yr^{-1}. For this reason, they become an influential factor of tip-AGB stellar evolution – but also vice versa, since our mass-loss rates vary strongly with effective temperature ($\dot{M} \propto T_{\rm eff}^{-8}$ (roughly), see Arndt et al. 1997), reflecting the temperature sensitivity of the dust formation process on a macroscopic scale.

With all tip-AGB models of an initial stellar mass $M_i \gtrsim 1.3 M_\odot$ we find superwinds with a total mass outflow of 0.26 to $\gtrsim 0.55 M_\odot$ during their final $3 \cdot 10^4$ yrs, just as required for PN-formation. Furthermore, a thermal pulse leads to a very short (100 to 200 yrs) interruption of the "superwind" of these models.

A critical (Eddington-like) luminosity L_c is required for the radiation driven wind models, which our evolution models fail to reach for $M_i \lesssim 1.1 M_\odot$. With slightly larger stellar masses, $L_{\rm tAGB}$ is near L_c and thermal pulses can trigger very short "superwind" bursts, as already pointed out by Schröder et al. (1998). We find good agreement between our improved models and the mass-loss characteristics of the thin CO shells found by Olofsson et al. (1990, 1993, 1996, 1998) around some carbon-rich Mira stars.

Key words: stars: carbon – stars: circumstellar matter – stars: evolution – stars: interiors – stars: late-type – stars: mass-loss

Send offprint requests to: K.-P. Schröder (schroder@ast.cam.ac.uk)

1. Introduction

Theoretical models of tip-AGB mass-loss (or "superwinds") are of considerable interest in several respects: from the stellar evolution point of view; for the understanding of the structure of circumstellar envelopes (CSE) and planetary nebulae (PN); and for the chemical evolution of the Galaxy and galaxies in general.

The term "superwind" has been coined to describe the heavy, final tip-AGB mass-loss ($\gtrsim 10^{-5} M_\odot$ yr^{-1}), which is required to form a PN of typically a few tenths of a solar mass (Peimbert 1981) within several 10^4 yr. It is supposed to develop rather gradually, by an accelerating increase of AGB mass loss, from a long history of less massive winds (e.g., Lafon & Berruyer 1991). Such a picture is in good agreement with the findings of cool, dust- and CO-rich CSE's around PNe (Kwok 1981) and the mass-loss rates of about 10^{-4} $M_\odot$ yr^{-1} as modeled on LPV (long period variable) observations (e.g., Knapp & Morris 1985, Winters et al. 1997).

While the general picture of PN formation is now certainly understood, well observed details of that process still await an explanation by more detailed models of the tip-AGB evolution and superwind mass-loss. We may remind of the well-known outer shells found around PNe in deep exposures (e.g., Guerrero et al. 1998). A probably related phenomenon seem to be the thin, detached CO shells found by Olofsson et al. (1990, 1993, 1996) for a few carbon stars, with kinematic ages of 3 to 13 thousand years and masses of 0.004 to $0.05 \cdot 10^{-2}$ $M_\odot$. These shells are reminiscent of very short episodes of a superwind which are contrasting the presently two orders of magnitude less dense winds of those objects. Width/radius ($\Delta R/R$) measurements suggest mass-loss event durations of – at least apparently – less than 2 to 3 thousand years, in one case ($\Delta R/R \approx 0.04$, Olofsson et al. 1998) even only 500 years. The same authors suggest thermal pulses as a possible driving mechanism for these abrupt and strong mass-loss fluctuations. But previous tip-AGB evolution models, using a parameterized "superwind" prescription (see below), resulted in a by far too shallow variation of the mass-loss rate with the thermal pulse cycle (e.g., Vassiliadis & Wood 1993).

Not only does the mass-loss rate depend critically on the actual stellar parameters and thus on details of the stellar evolution – moreover, tip-AGB stellar evolution itself is shaped signifi-

cantly by the increasing superwind mass-loss. Hence, for the final 10^5 years of stellar life on the AGB, mass-loss and stellar evolution have to be computed hand in hand. Earlier contributions to this specific problem have been published by, e.g., Vassiliadis & Wood (1993) and Blöcker (1995). Both approaches use a parameterized mass-loss, according to the characteristics of a Bowen-type wind-model (Bowen 1988) – a period – mass-loss relationship – i.e., the mass-loss rate depends strongly on the surface gravity g. That leads to a gradual but strong enhancement of the tip-AGB mass-loss, in good agreement with observational evidence. Those simple wind-models fail, however, to treat the important problem of dust-formation, with its complex and highly temperature- and density-dependent physics and chemistry, in sufficient detail.

A much different approach to tip-AGB mass-loss has been achieved by a consistent treatment of a dust-induced wind generation – including the detailed description of hydrodynamics, thermodynamics, chemistry, radiative transfer, dust formation and growth (see Sedlmayr 1994, Sedlmayr & Winters 1997, for recent reviews). Based on such extensive computations, Fleischer et al. (1992) have introduced consistent dynamical wind models for pulsating, C-rich AGB stars. These are in good agreement with observed carbon star mass-losses (Le Bertre & Winters 1998). A large number of such models have already been computed for different stellar parameters, and certain characteristics have been deduced (Arndt et al. 1997). Consequently, we applied those mass-loss characteristics to tip-AGB stellar models and already our first computations lead to the formation of "superwinds" (see Fig. 4 in Schröder et al. 1998). However, for a critical stellar mass range, we also already found the occurrence of very short "superwind" bursts leading to the formation of the typical "detached shell" characteristics.

The very abrupt nature of that phenomenon suggested further improvements of our computations to avoid artificial effects. Hence, we here present our most recent results, which now model the formation of regular "superwinds" in a wider range of stellar masses, and we discuss the related consequences for the formation of CSE's and PNe.

2. The evolution code and our approach to the "superwind" problem

We use the most recent version of an evolution code as described by Pols et al. (1995, 1998, and see references therein), which is based on the original evolution program of Eggleton (1971, 1972, 1973). The essential features, in which this code differs from other evolution programs, are: (1) the use of a self-adaptive, non-Lagrangian mesh, (2) the treatment of both convective and semi-convective mixing as a diffusion process with a diffusion rate adopted as a function of $(\nabla_{\rm rad} - \nabla_{\rm ad})$ and (3) the simultaneous and implicit solution of both the stellar structure equations and the diffusion equations for the chemical composition.

These characteristics are advantageous especially for the evolved stages with one or two thin shell sources, and there is no need for an external redistribution of mesh-points. All that makes the code easy to use, economic and robust. Furthermore, the Eggleton code easily accepts a significant mass-loss as part of the boundary condition. The trade-off for the robustness of the code in its present version is, however, that it cannot compute reliable surface abundance changes through dredge-up's: Thermal pulses are picked up on the AGB only far beyond their likely onset as it is suggested by other codes.

We checked the cycle times of our thermal pulses which, by a first comparison to other computations (e.g., Vassiliadis & Wood 1993), seem to be shorter. However, the thermal pulse cycle time is not as constant a quantity as the early pulses may suggest. In the presence of significant mass-loss and a therefore rapidly dwindling envelope mass on the very tip-AGB – see Wagenhuber & Weiss (1994) for such computations, and their Fig. 1 in particular – the final thermal pulses are found in much quicker succession than the early ones. Hence, since the Eggleton code computes thermal pulses only on the very tip-AGB, its short cycle times are not surprising.

Standard mixing-length theory is used to describe the heat transport. Consequently, the outer structure of the stellar models depends on the choice of α, which is the mixing length (ML) over the pressure scale height. On the other hand, the evolution of convective stellar cores (i.e., for $M_i \lesssim 1.5 M_\odot$) depends on the assumptions made with respect to any extended mixing or "overshooting". We here use the same set of parameters as discussed and recommended by Schröder (1998), and which are the result of a variety of critical tests by empirical methods (Schröder et al. 1997, Pols et al. 1997, Pols et al. 1998).

However, as with all other contemporary evolutionary codes which describe convective heat transport by the mixing-length theory and use a fixed ML parameter (here: $\alpha = 2.0$), the predicted GB and AGB effective temperatures are not very reliable, as pointed out by, e.g., VandenBerg 1991. Hence, in order to be more consistent with observed effective temperatures of tip-AGB objects (see, e.g., Van Belle et al. 1997), the Eggleton code requires a gradually decreasing α on the AGB, which reaches 1.5 at $\log g$ (cgs) $= -1$. Accordingly we have adopted $\alpha = 2.0 + 0.17 \cdot (\log g - 1.94)$ for $\log g < 1.94$. This can be regarded as an economical compensation for the combined effects on $T_{\rm eff}$ of a few common short-comings, such as the mixing length theory itself or incomplete opacities.

To incorporate realistic superwind mass-loss rates, we use analytic representations of $\dot{M}$ as a function of stellar effective temperature, luminosity and mass. These were obtained from a large number of detailed wind-model computations as described by Fleischer et al. (1992). There is not only a significant inverse dependence of Fleischer-type mass-losses on stellar mass, but much more strongly on effective temperature (already pointed out by Wagenhuber, 1996). This temperature sensitivity has its origin in the temperature-critical micro-physics and chemistry of the dust formation process (i.e., the grain nucleation rate) and is a characteristic property which we expect from any truely detailed model of a wind driven by radiation pressure on dust.

From a grid of 48 detailed wind models, Arndt et al. (1997) derived an approximative mass-loss formula for the tip-AGB region of the HR diagram which we have adopted for our com-

Table 1. Parameters and resultant quantities of some dust shell models in the critical parameter range. T_* and L_* refer to the hydrostatic initial model. The values of the remaining parameters are: carbon-to-oxygen ratio $\epsilon_{\rm C}/\epsilon_{\rm O} = 1.30$, Period $P = 400$d, and piston amplitude $\Delta u_p = 5\,{\rm kms}^{-1}$.

Model	M_* $[M_\odot]$	T_* [K]	L_* $[10^4 L_\odot]$	$< \dot{M} >$ $M_\odot\,{\rm yr}^{-1}$	$< v_\infty >$ $[{\rm kms}^{-1}]$
W45[1]	0.8	2600	0.3	$5.7\,10^{-7}$	2.0
W84[1]	1.2	2600	0.5	$4.3\,10^{-7}$	3.0
W46	0.8	2600	0.4	$5.7\,10^{-6}$	6.0
W83	1.2	2600	0.6	$6.5\,10^{-6}$	4.2
W47a[1]	0.8	3000	0.5	–	–
W54[1]	1.2	3000	1.2	$3.4\,10^{-8}$	2.9
W47	0.8	3000	0.6	$4.2\,10^{-6}$	10.0
W77	1.2	3000	1.4	$2.1\,10^{-7}$	5.7

[1]: below the critical limit; wind solution not always available

putations:

$$\log \dot{M} = 17.16\text{–}8.26 \cdot \log T_{\rm eff} + 1.53 \cdot \log L - 2.88 \cdot \log M$$

(see also Schröder et al. 1998); M, L in solar units, $T_{\rm eff}$ in K. As it turns out, this kind of mass-loss drives the tip-AGB star gradually into a rapidly increasing superwind ($\dot{M} > 10^{-5} M_\odot$/yr). However, since a minimum outward directed force is required to drive the wind, the star *also* needs to exceed a critical minimum (*Eddington-like*) luminosity L_c (see e.g. Sedlmayr & Winters 1997). In order to assess L_c from actual models, we computed a number of additional, critical wind models – see below.

3. L_c and recent computational improvements

Several improvements have been made with respect to our first computations (Schröder et al. 1998), through which our new models presented here differ in some details from earlier ones. In particular, L_c and the abrupt nature of the "superwind" bursts were given special consideration:

(1) A detailed consideration of the *Eddington-like* critical luminosity L_c, which can be the crucial factor for the onset of a dust-induced superwind: In general, any *purely radiation driven wind* requires

$$L_* > L_{\rm Edd} := \frac{4\pi c G M_*}{\chi_{\rm H}/\rho}$$

with c for speed of light, G for gravitation constant, M_* for actual stellar mass, ρ for mass density. In the case of our dust-induced winds, $\chi_{\rm H}$ is the flux-mean extinction coefficient of the dust component in the inner (dust forming) region.

For various reasons, only actual wind models can define $L_{\rm Edd}$ and its variation with effective temperature $T_{\rm eff}$ and M_*: The dust nucleation is extemely temperature-sensitve, whereas the grain growth process is mainly sensitive to density. Hence, $\chi_{\rm H}$ depends very sensitively on the local hydro- and thermodynamic conditions in the dust-formation zone, which in turn are governed by a strongly nonlinear equation system (see e.g. Sedlmayr & Winters 1997). Furthermore, an additional, outward force is introduced by the dissipation of shock wave momentum in our pulsating models, and our actual L_c-values are therefore a bit lower than $L_{\rm Edd}$.

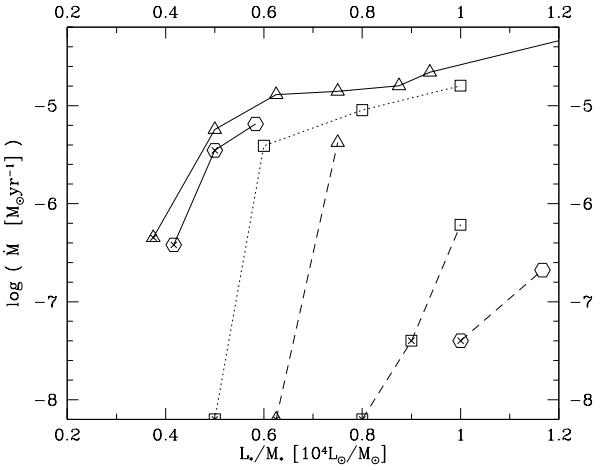

Fig. 1. Mass loss rates of our wind models as a function of L_*/M_* for several values of $T_{\rm eff}$ and M_*. Models of equal mass (triangles: $0.8 M_\odot$, squares: $1.0 M_\odot$, hexagons: $1.2 M_\odot$) are connected by different lines for different $T_{\rm eff}$ (solid lines: 2600K, dotted: 2800K, dashed: 3000K). A small cross inside a symbol indicates an outflow velocity below $5\,{\rm kms}^{-1}$. Models plotted on the bottom line have no wind solution at all.

For these reasons, we have computed a number of critical C-rich wind models (see Table 1 for a selection and Fig. 1). In Fig. 1 the resulting mass loss rates of wind models in the critical range are shown as a function of L_*/M_* for several stellar temperatures T_* and masses M_*. The models indicated at the bottom line ($\log \dot{M} = -8.2$) do not have a wind solution at all. Fig. 1 shows that there is a steep decrease of the mass-loss rate and of the outflow velocity, once L_*/M_* falls short of some critical value L_c/M_*. The sensitive variation of the corresponding critical luminosity L_c with stellar temperature and stellar mass represents, on a macroscopic scale, the non-linearity of the microscopic interaction between the dust-formation chemistry and the radiative transfer in our models. We find stable, massive winds (mostly, $\dot{M} \gtrsim 10^{-6} M_\odot\,{\rm yr}^{-1}$), which arrive at about the rates given by our aforementioned formula, above a line in the HRD running through $L_c \approx 5000 L_\odot \cdot M_*/M_\odot$ at $T_{\rm eff} = 2600K$, $L_c \approx 6000 L_\odot \cdot M_*/M_\odot$ at $T_{\rm eff} = 2800K$, and $L_c \approx 10000 L_\odot \cdot M_*/M_\odot \cdot (M_*/M_\odot - 0.05)$ at $T_{\rm eff} = 3000K$, respectively. Below that line (i.e., for smaller L_*), wind velocities and mass loss rates become very small ($v_\infty \lesssim 5\,{\rm kms}^{-1}$, $\dot{M} \lesssim 1 \cdot 10^{-6} M_\odot\,{\rm yr}^{-1}$) – if a wind model can be obtained at all.

(2) A realistic, well constrained pre-tip-AGB mass-loss history has been given special attention: For $L_* < L_c$ we adopt (time-step by time-step) the smaller of the mass-loss rates suggested by (a) de Jager et al. (1988) and (b) by the "Reimers formula" with a reduced $\eta_{\rm RML} = 8 \cdot 10^{-14}$. The original value of $\eta_{\rm RML} = 4 \cdot 10^{-13}$, suggested by Reimers (1975) and used by us in earlier computations (Schröder et al. 1998), leads to too

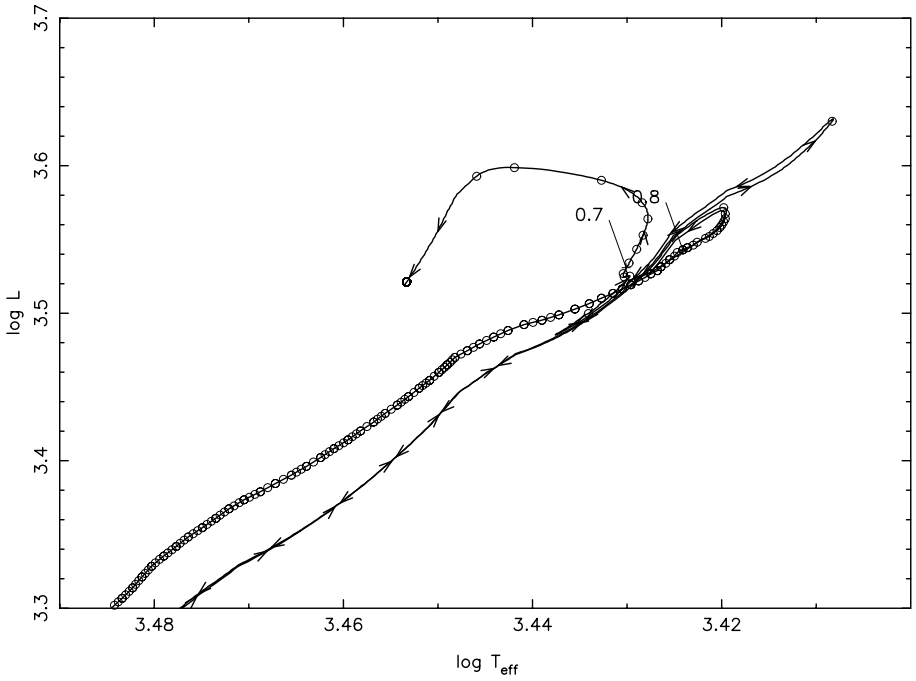

Fig. 2. The final, tip-AGB evolution of a star with an initial mass of 1.10 $M_\odot$ and about solar composition. Except for the one shown (the final one on the AGB), thermal pulses are suppressed. Circles mark time-steps of 5000 yr, arrows indicate direction of fast evolution and numbers mark the actual mass.

large RGB (red giant branch) mass-losses for our models with initial masses around $M_i \approx 1M_\odot$. Hence, we used those models as a sensitive constraint to our choice of $\eta_{\rm RML}$ – i.e., a RGB mass-loss $\gtrsim 0.4M_\odot$ would hinder a star of $M_i = 0.95M_\odot$ to reach He-burning and the horizontal branch. However, the more massive stars studied here for their tip-AGB mass-losses spend much less time on the RGB and their total RGB mass-loss is much less significant (see Table 2). – Our pre-tip-AGB mass-loss prescription is now also well in line with the more recent mass-loss rates derived from ζ Aur systems (Baade, 1998), from which $\eta_{\rm RML} \approx o(10^{-13})$ would be derived.

(3) A quick but *gradual* transition of the mass-loss rate at the onset of the "superwind": Below L_c, our models show a reduction of the mass-loss in a very small luminosity range (see Fig. 1). We therefore implemented a mass-loss ramp for $L_* < L_c$ with an appropriate width of 0.04 in $\log L_*$.

(4) Consistently reduced time-steps, when larger mass-loss rates occur, to keep the mass lost in each time-step well below $10^{-3}M_\odot$, and to avoid any artificial reaction of the stellar model, even under extreme conditions – i.e., as during a brief "superwind" burst.

(5) We found and removed an inconsistency between the prescribed mass-loss rate and the actual wind-models, which is of some significance to the superwind peaks and bursts: the respective mass-loss rates obtained from earlier computations (Schröder et al. 1998) were a bit too large.

(6) In order to resolve the rôle of stellar mass properly, we have extended the computations to form a consistent set of evolutionary models, in the mass range of $M_i = 1.0$ to 2.5 $M_\odot$, with a spacing of M_i as fine as (partly) $0.05M_\odot$. All models start from the zero age main sequence (ZAMS) with the same set of parameters as described above. We here present and discuss a representative selection of models from that set.

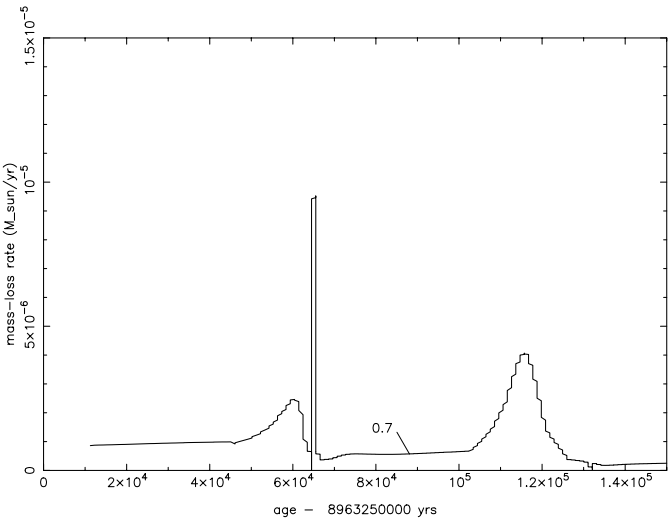

Fig. 3. Tip-AGB mass-loss history for the evolution model ($M_i = 1.10M_\odot$) shown in Fig. 2. Actual masses are marked by numbers. When such a star briefly reaches the critical luminosity on the tip-AGB with its last thermal pulse on the AGB, a short (about 800 yr) burst of superwind occurs.

4. $M_i = 1.1$ to $\approx 1.3M_\odot$: the formation of episodic "superwind" bursts

In this range of initial stellar mass, the tip-AGB luminosity $L_{\rm tAGB}$ reaches L_c, but only just and only briefly. The stellar model is driven into and out of the "superwind" mass-loss by its last one or two thermal pulses on the AGB. The response of the then very thin ($\lesssim 0.2M_\odot$) stellar shell to thermal pulses, especially in luminosity, is very pronounced, and both gravity and $T_{\rm eff}$ are very low. This results in short bursts and episodes of superwind (see Figs. 3 and 4), as already reported in a recent

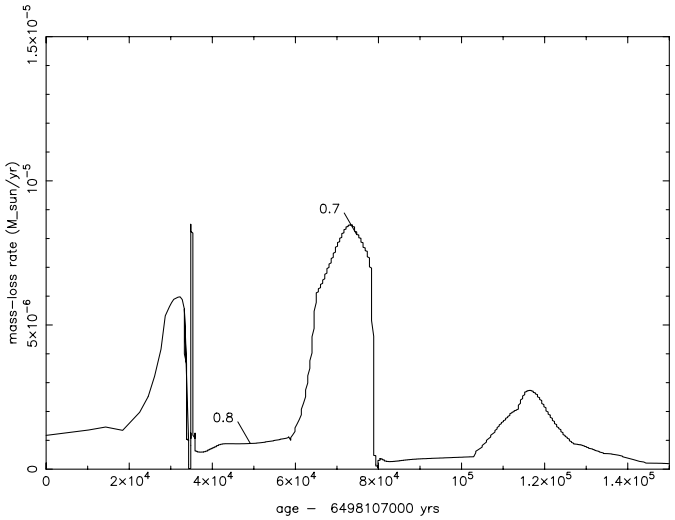

Fig. 4. Tip-AGB mass-loss history for a 1.20 $M_\odot$ (initial) mass star. Thermal pulse induced luminosity variations near L_c result in three mass-loss events in the course of $7 \cdot 10^4$ yr.

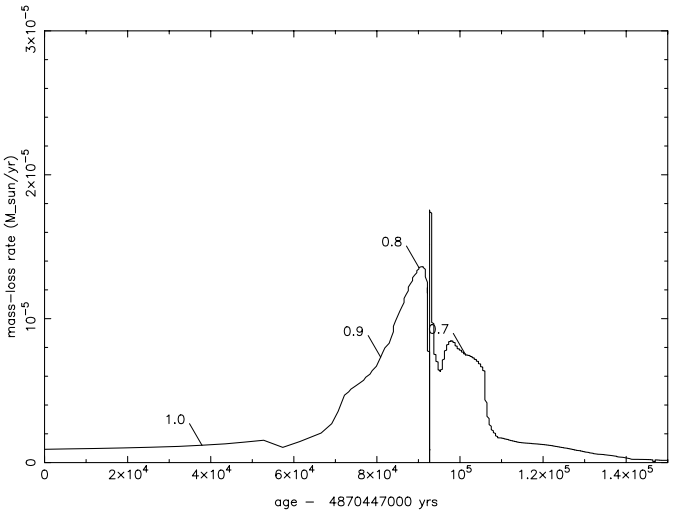

Fig. 5. The final, tip-AGB mass-loss history for a 1.30 $M_\odot$ (initial) mass star. The larger tip-AGB luminosity now exceeds L_c during the whole "superwind" phase. The only interruption is for just 200 yrs during a thermal pulse.

publication (Schröder et al. 1998), with durations ranging from about 800 years to several thousand years.

To arrive at more detailed results under realistic physical assumptions, our new computations comprise the improvements described in the previous section. Of these, three are of specific importance here: (1) the much better probed $L_c(T_{\rm eff})$, (2) using a 0.04 dex wide ramp in $\log L$ for a gradual transition into the superwind, and (3) much smaller time-steps with large mass-loss rates.

Consequently, we can now draw a more accurate and detailed picture of the dramatic changes of mass-loss in this range of initial stellar mass than Schröder et al. (1998): The lowest mass model ($M_i = 1.1 M_\odot$), which reaches L_c only marginally and only very briefly, is plotted in Fig. 2, its mass-loss history in Fig. 3: An isolated superwind burst is driven by the steep but very short (800 yr) luminosity peak immediately after the last thermal pulse on the tip-AGB, during the re-ignition of the H-burning shell. The actual stellar mass is already reduced to 0.72 $M_\odot$, with only $0.16\ M_\odot$ envelope mass left. These circumstances result in a much more immediate and pronounced response of the star than with the earlier thermal pulses – i.e., in a quick change of its surface luminosity and effective temperature with any variation of the H-burning shell energy production.

The resulting superwind burst removes 0.008 $M_\odot$ within 800 years, at a rate of $1 \cdot 10^{-5} M_\odot\,{\rm yr}^{-1}$. That falls well into the range of mass-loss characteristics found with geometrically thin, detached shells (CO observations by Olofsson et al. 1990, 1993, 1996, 1998). Furthermore, for L_* sufficiently larger than L_c, our superwind models suggest shell expansion velocities between 12 and 25 $\rm kms^{-1}$ (see Fleischer et al. 1992 and Arndt et al. 1997), which also agree well with the observed shell expansion velocities (13–20 $\rm kms^{-1}$, Olofsson et al. 1996).

By contrast, for $L_* \lesssim L_c$, our wind models suggest a very low wind velocity, of about or less than 5 $\rm kms^{-1}$ (see Table 1 and Fig. 1), which would consequently be our expectation for the wind of such a star after the ejection of a detached shell. In fact, this agrees well with the small present-day wind velocities found by Olofsson et al. (1996) for those carbon stars with a geometrically thin, detached shell.

Models with slightly increased M_i already probe L_c more easily, resulting in additional strong mass-loss events, removing several $10^{-2} M_\odot$ each – see Fig. 4 which shows the mass-loss history of a star with $M_i = 1.2 M_\odot$. Through the slow release of the energy from the thermal pulse (temporarily been stored in the envelope) plus the slowly growing H-burning shell luminosity, there is an enhanced – slow but significant – rise of luminosity until the next thermal pulse. Again, smaller envelope mass results in a more pronounced modulation of luminosity and drives the star into its second and third mass-loss event as seen in Fig. 4. The second event is ended by another thermal pulse, the third by the depletion of the stellar envelope: it finally starts to shrink and to increase $T_{\rm eff}$, so that the star leaves the superwind regime.

A typical mass-loss event duration in Fig. 4 is several thousand years. For a realistic age of 10^4 yr and with the assumption of a continuous outflow, this would lead to a somewhat extended detached shell ($\Delta R/R \approx 1/3$). If the density contrast can be enhanced by sweeping up the slower, previously emitted wind (when L_* was $\lesssim L_c$), such a shell may also, eventually, become geometrically thin.

5. $M_i \geq 1.3$: characteristic mass-loss histories of a dust-induced "superwind"

From $M_i \approx 1.3 M_\odot$ onwards, all evolution models yield a fairly similar tip-AGB superwind mass-loss record of the final $3 \cdot 10^4$ years. The superwind duration and the total mass lost in that phase varies in the realistic range of 0.26 $M_\odot$ ($M_i = 1.3 M_\odot$) to 0.55 $M_\odot$ ($M_i = 2.25 M_\odot$), see Table 2. Episodic mass loss

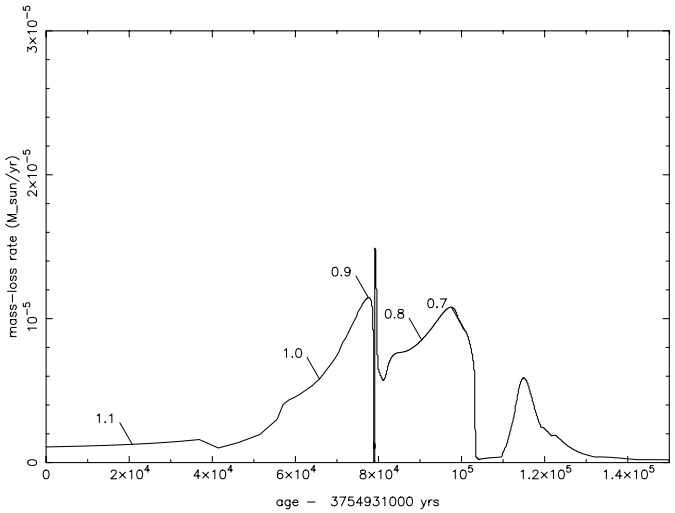

Fig. 6. Tip-AGB mass-loss history for a 1.40 $M_\odot$ (initial) mass star. This model suggests that some revived mass-loss can occur after the main "superwind"-phase has already ended, caused by the luminosity release from the last thermal pulse on the tip-AGB.

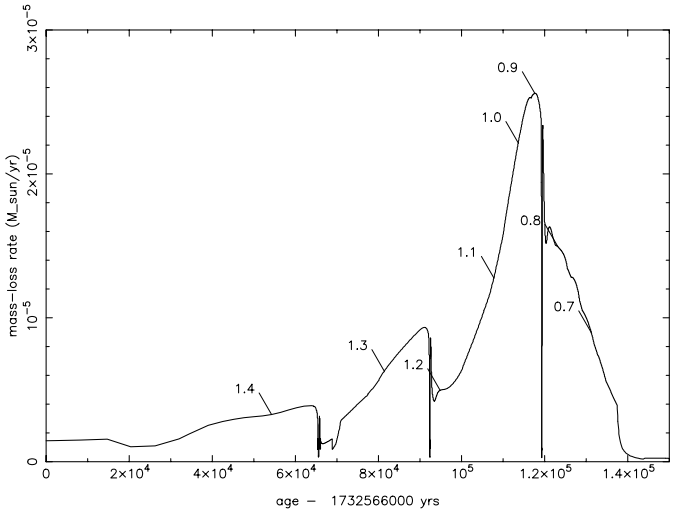

Fig. 7. Tip-AGB mass-loss history for a 1.85 $M_\odot$ (initial) mass star (see also Fig. 9). The mass-loss history of all these more massive models is strongly influenced by the strong temperature dependence of the "superwind".

events or bursts of superwind do not occur for $M_i > 1.4M_\odot$ (see the mass-loss histories shown in Figs. 5 to 8).

However, during the brief drop of luminosity during each thermal pulse, combined with an increased $T_{\rm eff}$ (see Fig. 9), for only 100 to 200 years, the mass-loss rate is reduced by 1 to 2 orders of magnitude. That strong contrast is the result of the strong luminosity and temperature sensitivity of the dust-induced mass-loss. Again there is matching evidence from detached shell observations, which suggest mass-loss interruptions at similar time scales – see Hashimoto et al. (1995, 1998) for a reported case with an O-rich Mira star, and Bagnulo et al. (1997) for a reported case with a carbon star.

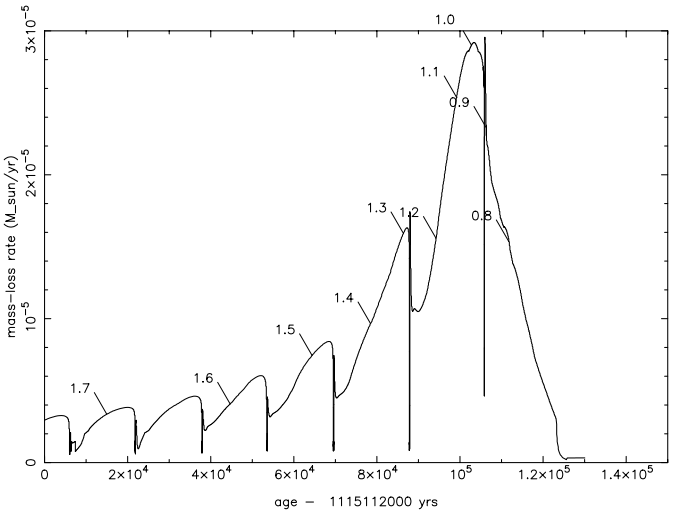

Fig. 8. Tip-AGB mass-loss history for a star with $M_i = 2.25M_\odot$.

With increasing M_i, several characteristics of the mass-loss history are changing gradually (see also Table 2):

(1) The integrated mass loss on the RGB becomes negligible, mainly because of the accelerated RGB evolution with increasing M_i. While 0.13 $M_\odot$ are lost on the RGB for $M_i = 1.10M_\odot$, this figure is reduced to 0.08 $M_\odot$ for $M_i = 1.30M_\odot$ and becomes less than 0.02 $M_\odot$ for $M_i \gtrsim 1.85M_\odot$.

(2) For $M_i \gtrsim 1.5M_\odot$, in contrast to the lower mass evolution models, a superwind does not start yet at L_c. Rather, those wind-model mass-losses start with about $o(10^{-6})$ $M_\odot$ yr^{-1}. Rates qualified for a superwind, i.e., $\dot{M} \geq 10^{-5}M_\odot$ yr^{-1}, are reached only *gradually* (apart from their modulation by thermal pulses) and later on the tip-AGB, with further decreasing $T_{\rm eff}$ and stellar mass (see Figs. 7 and 8).

(3) It is the sensitive dependence of our wind models on $T_{\rm eff}$ which strongly shapes the superwind mass-loss histories of stars with larger masses. It also leads to a gradual decline of $\dot{M}$ near the end of the superwind phase – by contrast to models with a conventional superwind prescription (see Fig. 10). This is caused by the rise of $T_{\rm eff}$ in the early turn-off from the tip-AGB, when only about 0.1 $M_\odot$ depleted envelope mass is left to lose towards the exposure of the hot stellar core. From this result, we expect consequences for the density profiles of CSE's and proto-PNe – i.e., the inner edge density gradients of undisturbed, cool envelopes should be not as steep as predicted by a conventional superwind model.

(4) At any given tip-AGB luminosity, models with larger M_i yield larger actual stellar masses M_* and slightly larger $T_{\rm eff}$ than their less massive counterparts. Hence, at any point on the tip-AGB, mass-loss rates drop quickly with increasing stellar mass.

With so different stars evolving through such a narrow region of the HR diagram, it is not possible to derive a simple mass-loss – luminosity (or $\dot{M}$ – period) relationship for a comparison with the one suggested by observational data (e.g., see Groenewegen & Whitelock et al. 1996). Rather, for any given luminosity, there is a side by side of stars with different mass and,

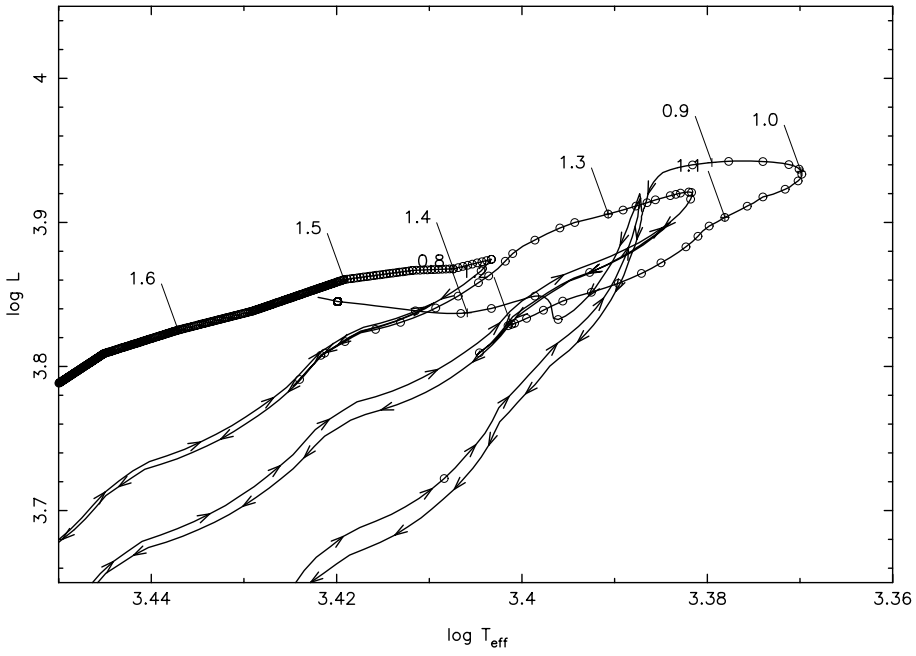

Fig. 9. The much more luminous tip-AGB evolution of a star with an initial mass of 1.85 $M_\odot$. Circles mark time-steps of 1000 yr. Thermal pulses prior to the 5 shown here are suppressed.

Table 2. Basic properties of selected evolution models: initial stellar mass M_i, M_{bgHe} (stellar mass at the begin of He burning), M_{bgSW} (at the "begin" of the "superwind", taken to be 30 000 years before the end), ΔM_{SW} (total "superwind" mass loss, by the same definition), and final stellar mass M_f, all given in $M_\odot$. The occurrence of an episodic mass loss event (EML) is indicated by an asterisk. (B) indicates use of a different "superwind", i.e., after Blöcker (see text).

M_i	M_{bgHe}	M_{bgSW}	ΔM_{SW}	M_f	EML
1.10	0.97	0.72	0.01	0.58	*
1.20	1.11	0.85	0.09	0.59	**
1.30	1.22	0.92	0.26	0.60	
1.40	1.33	0.97	0.28	0.61	(*)
1.85	1.83	1.14	0.48	0.65	
1.85	1.83	1.19	0.50	0.65	(B)
2.25	2.25	1.29	0.55	0.69	

consequently, different phase of mass-loss: At the same luminosity, at which less massive stars are found in their superwind phase, there are also some more massive stars which experience much lower, pre-superwind mass-loss rates. However, the superwind phase of the less massive stars is much shorter (by one to two orders of magnitude) than the pre-superwind phase of the more massive stars. For that reason, any present-day stellar sample with $\log L \lesssim 4$ should mainly show pre-superwind mass-losses. Only above $\log L \approx 4$, we expect that most stars have reached their L_c and should predominantly show superwind mass-losses.

According to Groenewegen et al. (1998), the average carbon star mass-loss rate starts to qualify for a superwind at $\log L = 4$, where it reaches $10^{-5} M_\odot$ yr^{-1} according to their empirical $\dot{M}$ – L_* relation. With the above said, this is in good agreement with the set of our computed mass-loss histories.

Finally, we like to point out that the final masses M_f of our models, as listed in Table 2, compare well with the empirically determined $M_f - M_i$ relationship as given by the detailed study of Weidemann (1987) – see, in particular, Fig. 1 therein.

6. Discussion

We consider this work as a first step to combine the so far separate worlds of stellar evolution models and detailed, self-consistent models of dust-driven winds to compute the final tip-AGB evolution and mass-loss history. Despite the large complexity involved on both a macroscopic and a microscopic scale, with numerous different physical and chemical processes networking together in a pulsating, C-rich dust-induced "superwind", there is excellent agreement between our computations and a variety of observational facts – i.e., outer shell structure found in deep exposures of PNe and, in particular, for detached circumstellar shells and envelopes. These features are, on a macroscopic scale, the direct consequence of the complex and temperature sensitive micro-physics, dust-formation chemistry and radiative transfer – leading, in particular, to (1) a $T_{\rm eff}$ and mass dependent critical luminosity L_c and (2) a mass-loss rate which is strongly $T_{\rm eff}$-sensitive.

We should mention here, that our wind models are subject to a simulated stellar pulsation as inner boundary condition and therefore include some mechanical energy and momentum input. Its exact description has some influence on the details of our wind models, but the mass-loss rate itself does not change much with the choice of pulsation parameters since the driving mechanism of the wind is radiation pressure on dust – the dust formation begins already deep inside the wind acceleration region, in the sub-sonic regime.

In that respect it is interesting to compare, all other model assumptions left unchanged, a mass-loss history of our dust-

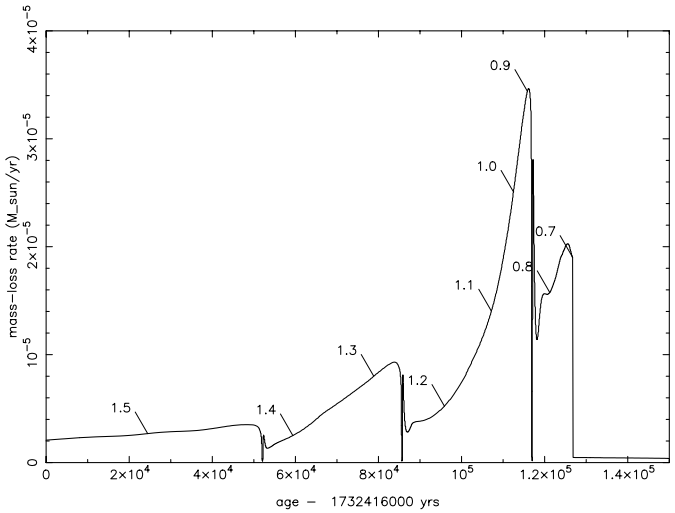

Fig. 10. Tip-AGB mass-loss history for a star with $M_i = 1.85 M_\odot$ with a conventional "superwind"-prescription according to Blöcker (1995), with $\eta = 0.1$. This "superwind" is much more gravity sensitive. Hence, it increases more rapidly and shows an abrupt end (compare to Fig. 7).

driven superwind to one which results from a conventional superwind prescription, i.e., as based on a simple pulsation-driven wind model. For that purpose, we choose the mass-loss formula adopted by Blöcker (1995) for a Bowen-type wind (Bowen 1988):

$$\log \dot{M} = \log \eta_B - 2.0 \cdot \log T_{\rm eff} + 4.2 \cdot \log L - 3.1 \cdot \log M - 13.2$$

We adopted $\eta_B = 0.1$ according to Groenewegen et al. (1995). Fig. 10 shows the resulting mass-loss history for the otherwise same 1.85 $M_\odot$ model shown in Figs. 7 and 9 – also, see the respective entries in Table 2. As can already be seen from the above formula, the "Blöcker"-wind is much more sensitive to surface gravity, but much less sensitive to $T_{\rm eff}$, when compared to our mass-loss rates. As a result, the mass-loss rate increases faster and removes slightly more mass in a shorter time, until it ends abruptly. By contrast, most evolution models with our temperature dependent mass-loss predict a gradual decline prior to the end of the superwind. Abrupt changes occur only in critical circumstances – i.e., when the luminosity is close to the critical luminosity of the wind model.

A sudden exposure of the stellar core is expected from an observational point of view, i.e. with respect to the small observed PN ages found in several cases. Our evolution code may not be detailed enough to give a reliable coverage of the very end of the superwind – instabilities, (e.g. by a sudden hydrogen recombination in the shell (Wagenhuber & Weiss 1994)) are not considered here. On the other hand, as already pointed out by Pottasch (1984), such observed PN ages could turn out to be significantly underestimated, if the main CSE mass lies outside the visible PN. That would be the case if the final superwind mass-loss is reduced, just as suggested by our models.

Hence, it is difficult to decide, which of the two alternatives comes closer to the truth: a quick turn-off from the tip-AGB as with a strongly gravity-sensitive superwind, or a slower turn-off as could be expected from a predominantly $T_{\rm eff}$-sensitive, dust-induced superwind. Because of its dramatic implications for the post-AGB evolution, this issue still remains an important open question for future research on CSE's and PNe.

With the strong temperature-dependence of the mass-loss rate in mind, we have to re-consider our adjustment of the mixing length on the AGB – is it critical? Counter the first impression, a slightly different tip-AGB α does in fact not matter much, as long as the tip-AGB reaches the dust-forming region of the HRD at all. If the evolutionary track, e.g., is shifted slightly to larger $T_{\rm eff}$'s, then all what happens is that the model evolves to slightly higher luminosities before the superwind sets in, with a very similar mass-loss history. Because of the core-mass – luminosity relation on the tip-AGB, the star will arrive at slightly higher core masses and thus somewhat larger M_f's. In relative terms, however, that makes not much difference to the total mass lost during the C-rich (super)wind phase.

Another critical point remains to be inspected: since the present version of our evolution code does not compute mixing associated with the dredge-up's, we cannot use the actual C:O surface ratio of our stellar models as a quantity to define the mass-loss rate in a strictly self-consistent way, but have to seek observational evidence instead. For example, the assumption of C-rich winds implies that a C:O ratio > 1 is reached *before* L reaches L_c. In fact, observational data suggest that carbon stars are already found with luminosities from around or slightly below the lowest L_c possible, which is (with a tip-AGB stellar mass of 0.75 $M_\odot$) $\log L \approx 3.6$ or $\rm M_{bol} \approx -4.3$. With the period-luminosity relation derived by Groenewegen & Whitelock (1996), this translates into periods of about 265 days. In fact, periods of well observed carbon stars start with 252 and 297 days (Groenewegen et al. 1998), and the bulk of carbon star $\rm M_{bol}$ values derived from $Hipparcos$ parallax's (Alksnis et al. 1998) starts from about -3.7.

All our wind models, from which we have derived L_c and $\dot{M}$, were computed with C:O ratios starting from 1.3. That appears to be in some contradiction to the expectation that C:O values should be just above 1 at the onset of carbon star winds. However, our models rather *under*estimate the dust-formation, caused by the limited representation of the large number of complex chemical reactions, and therefore the models might require a slightly too large C:O value for compensation. Also, our models assume 100% oxygen blocking by the CO molecule, which again is on the conservative side. With a more partial C-O blocking, a smaller C:O ratio would suffice with our wind models to yield the same wind properties.

Once a C-rich, dust-induced wind is finally established, it is, as our computations show (see, e.g. Arndt et al. 1997), almost independent of the C:O ratio. For all the above given reasons, we do not consider the lack of consistency with the C:O ratio as a critical issue.

Conclusions

Our models of the crucial final tip-AGB stellar evolution with strong mass-loss are in excellent agreement with a variety of points based on observational insight:

(1) We find regular "superwinds", with the exact characteristics required for PN formation, at the tip-AGB of all evolutionary models with $M_i \gtrsim 1.3 M_\odot$. It is mainly the strong temperature dependence of the micro-physics and dust-formation chemistry, which drives the superwind into increasingly larger mass-loss rates, while the gravity dependence assists but does not dominate the process – in contrast to the conventional Bowen-type "superwind" prescription.
(2) Our computations suggest realistic PN masses, i.e., between 0.26 to $\gtrsim 0.55\ M_\odot$, for a wide range of initial stellar masses ($1.3\ M_\odot$ to $2.5\ M_\odot$). Furthermore, the final masses of the stellar remnants agree well with empirical $M_f - M_i$ data.
(3) The existence of a critical luminosity L_c as a decisive factor for the mass loss mechanism, which – in connection with a thermal pulse – triggers brief superwind bursts for stars with $M_i \approx 1.1$ to $1.25\ M_\odot$, is confirmed by a striking coincidence between our models and recent high spatial resolution CO observations of thin detached shells around a few carbon stars.

Acknowledgements. This work has been supported by the DFG grants Se 420/12-1 and Se 420/8-1, and by the BMBF grant 05 3BT13A 6. The calculations of the wind models were performed on the CRAY computers of the Konrad-Zuse-Zentrum für Informationstechnik Berlin (ZIB). Subsequent data analysis has been performed on the WAP–cluster of the physics department of the TU–Berlin. We are grateful to P.P. Eggleton (IoA Cambridge) for providing his evolutionary code to us. We also thank D. Schönberner (IAP, Potsdam) for some very helpful suggestions, and the anonymous referee for valuable comments.

References

Alksnis A., Balklavs A., Dzervitis U., Eglitis I., 1998, A&A 338, 209
Arndt T.U., Fleischer A.J., Sedlmayr E., 1997, A&A 327, 614
Baade R., 1998, In: Harris B. (ed.) Ultraviolet Astrophysics. Beyond the IUE Final Archive. ESA SP-413, 325
Bagnulo S., Skinner C.J., Doyle J.G., Camphens M., 1997, A&A 321, 605
Blöcker T., 1995, A&A 297, 727
Bowen G.H., 1988, ApJ 329, 299
de Jager C., Nieuwenhuijzen H., van der Hucht K.A., 1988, A&AS 72, 259
Eggleton P.P., 1971, MNRAS 151, 351
Eggleton P.P., 1972, MNRAS 156, 361
Eggleton P.P., 1973, MNRAS 163, 179
Fleischer A.J., Gauger A., Sedlmayr E., 1992, A&A 266, 321
Guerrero M.A., Villaver E., Manchado A., 1998, ApJ 507, 889
Groenewegen M.A.T., van den Hoek L.B., de Jong T., 1995, A&A 293, 381
Groenewegen M.A.T., Whitelock P.A., 1996, MNRAS 281, 1347
Groenewegen M.A.T., Whitelock P.A., Smith C.H., Kerschbaum F., 1998, MNRAS 293, 18
Hashimoto O., Izumiura H., Kester D.J.M., Bontekoe Tj.R., 1995, Ap&SS 224, 477
Hashimoto O., Izumiura H., Kester D.J.M., Bontekoe Tj.R., 1998, A&A 329, 213
Knapp G.R., Morris M., 1985, ApJ 292, 640
Kwok S., 1981, In: Iben Jr. I., Renzini A. (eds.) Physical Processes in Red Giants. D. Reidel Publ. Co., Dordrecht, Holland, 421
Lafon J.-P.J., Berruyer N., 1991, A&AR 2, 249
Le Bertre T., Winters J.M., 1998, A&A 334, 173
Olofsson H., Carlström U., Eriksson K., Gustafsson B., Willson L.A., 1990, A&A 230, L13
Olofsson H., Eriksson K., Gustafsson B., Carlström U., 1993, ApJS 87, 267
Olofsson H., Bergman P., Eriksson K., Gustafsson B., 1996, A&A 311, 587
Olofsson H., Bergman P., Lucas R., et al., 1998, A&A 330, L1
Peimbert M., 1981, In: Iben Jr. I., Renzini A. (eds.) Physical Processes in Red Giants. D. Reidel Publ. Co., Dordrecht, Holland, 409
Pols O.R., Tout C.A., Eggleton P.P., Han Z., 1995, MNRAS 274, 964
Pols O.R., Tout C.A., Schröder K.-P., Eggleton P.P., Manner J., 1997, MNRAS 289, 869
Pols O.R., Schröder K.-P., Tout C.A., Hurley J.R., Eggleton P.P., 1998, MNRAS 298, 525
Pottasch S.R., 1984, Planetary Nebulae. Astrophysics & Space Science Library, D. Reidel Publ. Co., Dordrecht, Holland, 107
Reimers D., 1975, In: Baschek B., Kegel W.H. (eds.) Problems in Stellar Atmospheres and Envelopes. Springer, Berlin, 229
Renzini A., 1981, In: Iben Jr. I., Renzini A. (eds.) Physical Processes in Red Giants. D. Reidel Publ. Co., Dordrecht, Holland, 431
Schröder K.-P., 1998, A&A 334, 901
Schröder K.-P., Pols O.R., Eggleton P.P., 1997, MNRAS 285, 696
Schröder K.-P., Winters J.M., Arndt T.U., Sedlmayr E., 1998, A&A 335, L9
Sedlmayr E., 1994, In: Jørgensen U.G. (ed.) IAU Colloquium 146: Molecules in the Stellar Environment. Springer–Verlag, Berlin, 163
Sedlmayr E., Winters J.M., 1997, Stellar Atmospheres: Theory and Observations. Lecture Notes in Physics Vol. 497, Springer, EADN Astrophysics School IX, 89
Van Belle G.T., Dyck H.M., Thompson R.R., Benson J.A., Kannappan S.J., 1997, AJ 114, 2150
VandenBerg D.A., 1991, In: James K. (ed.) ASP Conf. Ser. 13: The formation and evolution of star clusters. 183
Vassiliadis E., Wood P.R., 1993, ApJ 413, 641
Wagenhuber J., Weiss A., 1994, A&A 290, 807
Wagenhuber J., 1996, Ph.D.-Thesis, FB Physik of the TU München
Weidemann V., 1987, A&A 188, 74
Winters J.M., Fleischer A.J., Le Bertre T., Sedlmayr E., 1997, A&A 326, 305